BIOCHEMISTRY
including biophysical chemistry & molecular biology

Article

pubs.acs.org/biochemistry

Binding of Yeast Cytochrome *c* to Forty-Four Charge-Reversal Mutants of Yeast Cytochrome *c* Peroxidase: Isothermal Titration Calorimetry

James E. Erman,* Lidia B. Vitello, Naw May Pearl, Timothy Jacobson, Meka Francis, Erik Alberts, Allen Kou, and Kathy Bujarska

Department of Chemistry and Biochemistry, Northern Illinois University, DeKalb, Illinois 60115, United States

Supporting Information

ABSTRACT: Previously, we constructed, expressed, and purified 46 charge-reversal mutants of yeast cytochrome *c* peroxidase (CcP) and determined their electronic absorption spectra, their reaction with H_2O_2, and their steady-state catalytic properties [Pearl, N. M. et al. (2008) *Biochemistry 47*, 2766−2775]. Forty-four of the mutants involve the conversion of either an aspartate or glutamate residue to a lysine residue, while two are positive-to-negative mutations, R31E and K149D. In this paper, we report on a calorimetric study of the interaction of each charge-reversal mutant (excluding the internal mutants D76K and D235K) with recombinant yeast iso-1 ferricytochrome *c*(C102T) (yCc) under conditions where only one-to-one yCc/CcP complex formation is observed. Thirteen of the 44 surface-site charge-reversal mutants decrease the binding affinity for yCc by a factor of 2 or more. Eight of the 13 mutations (E32K, D33K, D34K, E35K, E118K, E201K, E290K, E291K) occur within, or on the immediate periphery, of the crystallographically defined yCc binding site [Pelletier, H. and Kraut, J. (1992) *Science 258*, 1748−1755], three of the mutations (D37K, E98K, E209K) are slightly removed from the crystallographic site, and two of the mutations (D165K, D241K) occur on the "back-side" of CcP. The current study is consistent with a model for yCc binding to CcP in which yCc binds predominantly near the region defined by crystallographic structure of the 1:1 yCc−CcP complex, whether as a stable electron-transfer active complex or as part of a dynamic encounter complex.

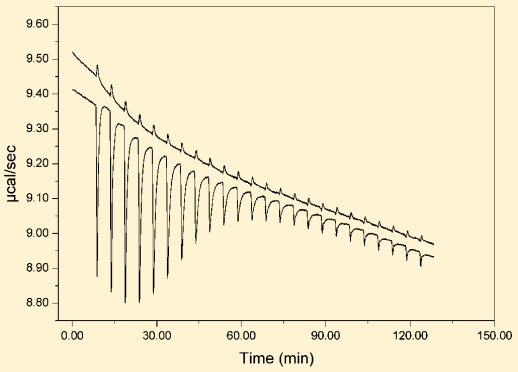

Yeast cytochrome *c* peroxidase (CcP) is a heme protein that reduces H_2O_2 to water utilizing two molecules of ferrocytochrome *c* (Cc^{2+}).[1] The net reaction is shown in eq 1.

$$2Cc^{2+} + H_2O_2 + 2H^+ \xrightarrow{CcP} 2Cc^{3+} + 2H_2O \quad (1)$$

The mechanism involves oxidation of the native ferric enzyme by H_2O_2 to an enzyme intermediate, CcP Compound I, which is oxidized two equivalents above the native state.[2] CcP Compound I is reduced back to the ferric state by two sequential electron transfer steps from Cc^{2+}. The electron transfer reactions involve complex formation between the two proteins.

Margolisah and co-workers were the first to suggest the possibility of multiple cytochrome *c* (Cc) binding sites on the surface of CcP.[3] They interpreted their biphasic steady-state velocity profiles in terms of both one-to-one (1:1) and two-to-one (2:1) Cc/CcP complexes. Mauk et al.[4] provided the first nonkinetic evidence for the existence of a 2:1 Cc/CcP complex in solution. Formation of the 1:1 complex has been shown to be strongly dependent on the ionic strength, while formation of the 2:1 complex, which is about 10^3-times weaker, is somewhat less dependent on ionic strength.[5]

Immediately after the determination of the crystal structure of CcP,[6,7] a hypothetical model for the Cc/CcP complex was proposed based on matching negatively charged residues on the surface of CcP with a group of conserved lysine residues that surround the exposed heme edge in Cc.[8−10] The hypothetical model suggested that Asp-33, Asp-37, and Asp-217 on CcP interacted with Lys-5, Arg-13, and Lys-72 on yeast iso-1 cytochrome *c* (yCc).[10] Subsequently Northrup and colleagues modeled the electrostatic interaction between Cc and CcP using Brownian dynamics simulations and identified three regions on the surface of CcP that had a high probability of forming productive electron-transfer complexes.[11] The three regions were located near Asp-34, Asp-148, and Asp-217.

In 1992, Pelletier and Kraut determined crystallographic structures of 1:1 complexes formed between horse Cc (hCc) and CcP and between yCc and CcP.[12] The 1:1 crystallographic complexes show that both hCc and yCc bind in a region between Asp-34 and Glu-290 on the surface of CcP, although in slightly different orientations. Horse Cc forms two discrete

Received: June 19, 2015
Revised: July 24, 2015
Published: July 25, 2015

ACS Publications © 2015 American Chemical Society

DOI: 10.1021/acs.biochem.5b00686
Biochemistry 2015, 54, 4845−4854

salt bridges with CcP in the complex; Lys-72 and Lys-87 on hCc interact with Glu-290 and Glu-35 on CcP, respectively. Although no salt bridges are seen in the yCc/CcP complex, small movements within the complex structure could produce salt bridges between lysine residues located at positions 73 and 87 in yCc with Glu-290 and Asp-34 on CcP, respectively.

The nature of the 1:1 and 2:1 complexes have been the subject of considerable interest. Two fundamentally different models for Cc/CcP binding have been proposed.[5,13−15] The first model is a unique sites model that postulates a unique high-affinity Cc-binding site and a single low-affinity binding site on the surface of CcP.[5] The second model postulates multiple binding sites on the surface of CcP with similar affinities for Cc.[13] The latter model assumes that the hCc/CcP and yCc/CcP structures seen in the crystalline state each represent one of the multiple 1:1 complexes that exist in solution, perhaps stabilized by the crystallization process. The second model also assumes that formation of the 2:1 complex is significantly weaker than formation of the 1:1 complexes due to electrostatic repulsion between bound cytochromes.

One way to distinguish between the two models is to map the surface of CcP that interacts with Cc under conditions where only 1:1 complex formation occurs (high ionic strength and low protein concentration). If the first model is correct, the interaction surface will be localized and in the region identified by the crystal structures of the 1:1 complexes. If the second model is correct, the interaction surface will be more extensive, including regions that are outside the crystallographically identified binding domain.

We have undertaken a project to map the yCc interaction sites on the surface of CcP in solution by using charge-reversal mutants of CcP. We hypothesize that if a negatively charged residue on the surface of CcP makes a significant contribution to binding yCc, changing that residue to a positively charged residue will lead to electrostatic repulsion and weakening of the interaction. On the other hand, if a negatively charged residue is not involved in binding yCc, charge-reversal on that residue will have little effect on binding. CcP contains 45 aspartate and glutamate residues, 42 of which have their carboxylates on the surface of the molecule and three of which have carboxylates buried within the protein.[7,16] The internal carboxylic acid residues are Glu-76, Asp-106, and Asp-235. We have used site-directed mutagenesis to convert the surface aspartate and glutamate residues, one at a time, to lysine residues, generating 42 negative-to-positive charge-reversal mutants. In addition, we have made two positive-to-negative mutations, Arg-31 to glutamate and Lys-149 to aspartate, both of which could potentially enhance yCc binding.

Previously, we have expressed and purified 46 charge-reversal mutants (including the internal mutants E76K and D235K) of CcP and determined their electronic absorption spectra, their reaction with H_2O_2, and their steady-state kinetic properties in the oxidation of yCc.[17,18] Interestingly, only 5 of 46 charge-reversal mutants significantly increased the Michaelis constant in the steady-state kinetic studies. Four of the mutants, R31E, D34K, E118K, and E290K occur within the cytochrome *c* binding site identified in the crystal structure of the 1:1 complex between yCc and CcP. The fifth mutation, D37K, lies outside, but near, the crystallographic site.

In this study, we report on the thermodynamic characterization of the interaction between yCc and 44 charge-reversal mutants of CcP using isothermal titration calorimetry (ITC) under conditions where only 1:1 complex formation is observed.

MATERIALS AND METHODS

Proteins. Construction of the CcP charge-reversal mutants, as well as the protocols for protein expression, purification, and concentration determination have been described previously.[17] Recombinant yeast iso-1 cytochrome *c*(C102T) was used for all binding experiments.[17] The Cys-102 to threonine mutation is used to prevent dimerization of the native cytochrome *c* via disulfide bond formation and has no effect on binding to CcP.

Buffer. The buffer was prepared by titrating 0.0567 M (final concentration) of dimethylglutaric acid (DMG) to pH 6.0 with KOH. The ionic strength of the buffer is 0.100 M. DMG is a dicarboxylic acid with thermodynamic (zero ionic strength) pK_a's of 3.73 ± 0.09 and 6.39 ± 0.13 at 25 °C.[19] Using the extended Debye−Hückel equation to estimate activity coefficients, the apparent pK_a's at 0.10 M ionic strength are 3.6 ± 0.1 and 6.2 ± 0.1.

Sample Preparation. Samples of yCc^{3+} (∼20 mg/mL) and the CcP mutants (∼2 mg/mL) were prepared in DMG buffer and dialyzed against 2 L of DMG buffer for 24 to 48 h at 4 °C to reach osmotic equilibrium. The samples were collected and centrifuged at 20 °C to remove insoluble material. The buffer used for dialysis was retained for the yCc dilution experiments. The pH of the buffer and protein samples after dialysis were generally within ±0.05 pH units of each other. Absorption spectra of the two dialyzed protein samples were obtained in order to determine the final protein concentration. Extinction coefficients for CcP and yCc^{3+} samples were 101 and 118 mM^{-1} cm^{-1}, respectively, both at 408 nm. Thirty minutes prior to each titration experiment, both the yCc and CcP samples were degassed under a vacuum.

Isothermal Titration Calorimetry (ITC). ITC experiments were performed using a MicroCal VPI isothermal titration calorimeter. CcP solutions were loaded into the calorimeter cell, and the yCc solution was loaded into the injection syringe. The sample was thermally equilibrated at 20 °C until a stable baseline was achieved. The experiment was initiated with a 2 μL injection of yCc into the reaction cell followed by up to an additional 27 injections, 10 μL each, of yCc. The syringe was rotated at 400 rpm for the duration of the experiment, and the time between injections was generally 300 s but some runs had intervals of up to 480 s. The temperature of the cooling-plates was maintained at 5 °C below the temperature of the reference and titration cells.

ITC Data Analysis. Data analysis was performed using software provided by MicroCal. The software allowed integration of the peak areas from each injection. The first injection was discarded due to possible diffusion of reactants into and out of the syringe tip during the initial thermal equilibration period. The integrated peak areas from a reference titration with yCc diluted into the buffer were subtracted from those of the protein/protein titrations in order to account for the enthalpy of dilution, small mismatches in the pH of the protein and buffer samples, and heats associated with the mechanical injection of titrant. The ITC analysis requires that the heat approach zero at infinite concentrations of the titrant, yCc. Occasionally, the heats did not approach zero after correction for the heats of dilution, and an additional correction to the titration was made by either adding or subtracting a small constant value of the heat selected to minimize the error in fitting the data. Corrected isotherms were fit to a single-site

DOI: 10.1021/acs.biochem.5b00686
Biochemistry 2015, 54, 4845−4854

binding-site model. The MicroCal-provided software uses nonlinear least-squares regression based on the Marquardt algorithm as described by Wiseman et al.[20] and Bevington.[21] Three parameters are used in the fitting procedure: the stoichiometric factor, n, the equilibrium association constant, K_{A1}, and the change in enthalpy, $\Delta H^{0\prime}$. The value of n may differ from unity in the single-binding-site model due to errors in protein concentrations, incorrect corrections for the reference titration, displacement of sample from the calorimeter cell during the titration, as well as other factors.

RESULTS

Binding of Recombinant CcP and Yeast Iso-1 Ferricytochrome c(C102T). Four isothermal calorimetric titrations were carried out using two different isolates of recombinant CcP (rCcP). The rCcP concentrations varied between 65.1 and 71.2 μM and the yCc concentrations ranged between 0.942 and 0.976 mM. Figure 1 shows one of the

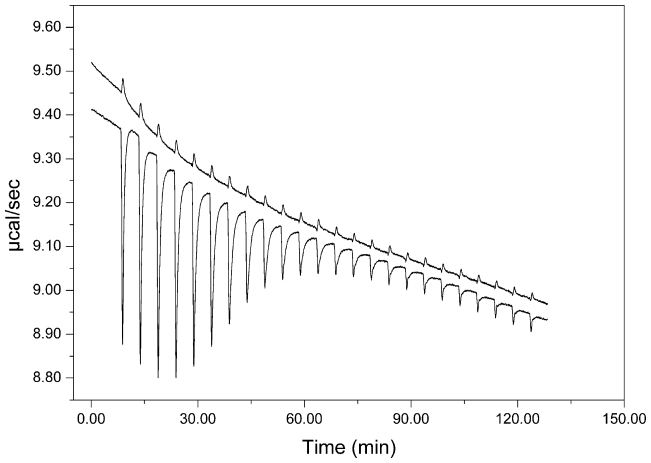

Figure 1. ITC titration of rCcP (65.1 μM) with yCc (0.976 mM) (lower trace) and yCc dilution (upper trace). Experimental conditions: 56 mM DMG buffer, pH 6.0, 0.100 M ionic strength, 20 °C.

titrations along with the corresponding yCc dilution. Figure 2 (open symbols) shows a plot of the observed heats, corrected for yCc dilution, as a function of the mole ratio of yCc to rCcP along with the best-fit line (dashed line) calculated from fitting the data to a single-binding-site model for the interaction between the two proteins.

Figures 1 and 2 illustrate one of the limitations of this study. Because of the small heats of binding in the yCc/CcP system, dilution effects can make substantial contributions to the observed heats during the protein−protein titrations, all of which may not be accounted for by using a single yCc dilution curve to correct the data. Replicate trials of yCc dilutions show small differences between runs. In addition, even after extended dialysis, the pH of the buffer, yCc, and CcP samples may differ by as much as 0.05 pH units, which also contributes to the error in using dilution experiments to correct the titration data. For the experiment shown in Figures 1 and 2, applying a small additional baseline corrections to the protein titration data to minimize the error in fitting the single-binding-site model improves the fit by about 40%, Figure 2 (solid symbols and solid line). The value of K_{A1} can vary by a factor of 2 depending upon the baseline correction procedure. In this study, we used the yCc dilution experiments to make the primary corrections to the protein titration data, then applied an additional baseline

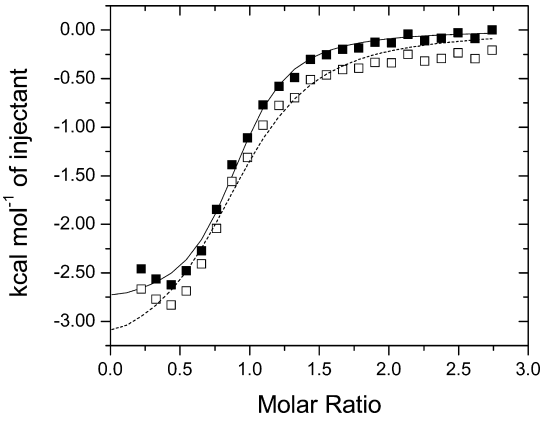

Figure 2. Integrated peak areas for the ITC titration shown in Figure 1 corrected for the yCc heat of dilution (open squares) and with an addition 156 cal/mol baseline correction (solid squares). Both sets of corrected data were fit to a single-binding-site model. The dashed line represents the best fit to the data shown in open circles and gives values for n, K_{A1}, and $\Delta H^{0\prime}$ of 0.92 ± 0.04, (1.5 ± 0.3) × 10^5 M^{-1}, and −3.4 ± 0.2 kcal/mol, respectively. The standard deviation of the experimental data from the dashed line is 126 cal/mol. The uncertainties in the parameters obtained from fitting individual titrations are estimated from the deviation of the data from the fitted line. The solid line shows the best-fit to the data shown in solid circles and gives best-fit values for n, K_{A1}, and $\Delta H^{0\prime}$ of 0.89 ± 0.02, (3.4 ± 0.5) × 10^5 M^{-1}, and −2.86 ± 0.08 kcal/mol, respectively. The standard deviation of the experimental data from the solid line is 74 cal/mol, a 40% improvement in fit.

correction, if necessary, to minimize the error in fitting the data to the single-binding-site model. The validity of the procedure is substantiated by the agreement of our data with previous thermodynamic studies of the interaction of yCc with CcP.

Fitting the four baseline-corrected ITC titrations for the rCcP/yCc interaction gives average values for n, K_{A1}, and $\Delta H^{0\prime}$ for the four titrations of 0.93 ± 0.03, (2.9 ± 0.7) × 10^5 M^{-1}, and −2.1 ± 0.8 kcal/mol, respectively, Table 1.

The values of K_{A1} and $\Delta H^{0\prime}$ obtained in this study are similar to previously reported values under similar, although not identical, experimental conditions. Wang and Pielak performed ITC experiments with authentic yeast cytochrome c and rCcP under a variety of conditions.[22] At pH 6.0, 20 °C, using a 50 mM DMG buffer (0.087 M ionic strength), Wang and Pielak report n, K_{A1}, and $\Delta H^{0\prime}$ values of 0.86 ± 0.02, (5.5 ± 2.9) × 10^5 M^{-1}, and −2.9 ± 0.1 kcal/mol, respectively. It is expected that binding will be stronger in the lower ionic strength buffer used by Wang and Pielak compared to the 0.100 M ionic strength buffer used in our study. To compare our data with that of Wang and Pielak we performed five titrations using 50 mM DMG buffer at 20 °C and found average values of 0.94 ± 0.01, (5.1 ± 0.3) × 10^5 M^{-1}, and −2.6 ± 0.1 kcal/mol for n, K_{A1}, and $\Delta H^{0\prime}$, respectively, essentially identical to the results of Wang and Pielak.

Mauk et al., 1994[4] used potentiometric methods to monitor the binding of yCc to rCcP in unbuffered solutions. Using 0.100 M KNO_3 as supporting electrolyte, Mauk and colleagues report K_{A1} values of (2.59 ± 0.08) × 10^5 and (2.46 ± 0.02) × 10^5 M^{-1} at 18 and 25 °C, respectively, at pH 5.99. Their value of K_{A1} is essentially independent of temperature between 18 and 25 °C, and within experimental error of our data at 0.100 M ionic strength, pH 6.0.

DOI: 10.1021/acs.biochem.5b00686
Biochemistry 2015, 54, 4845−4854

Table 1. Mutants with K_{A1} at Least a Factor of Two Smaller than K_{A1} for the yCc/rCcP Complex[a]

protein	number of titrations	n	10^{-5} K_{A1} (M^{-1})	$\Delta H^{0\prime}$ (kcal/mol)
rCcP	4	0.93 ± 0.03	2.9 ± 0.7	−2.1 ± 0.8
D34K	2		NDI[c]	NDI[c]
E201K	4		NDI[c]	NDI[c]
E290K	6		NDI[c]	NDI[c]
D33K	4	1[b]	0.04 ± 0.03	+2 ± 2
D37K	2	1[b]	0.11 ± 0.04	+0.28 ± 0.09
E118K	2	0.6 ± 0.1	0.19 ± 0.09	+0.6 ± 0.3
D241K	6	0.8 ± 0.6	0.21 ± 0.03	−9 ± 2
E209K	2	0.8 ± 0.1	0.4 ± 0.1	−5 ± 1
E291K	4	0.78 ± 0.05	0.6 ± 0.1	−3.2 ± 0.3
D165K	4	0.8 ± 0.3	0.8 ± 0.1	−2.8 ± 0.6
E32K	2	0.4 ± 0.2	0.82 ± 0.08	−1.9 ± 0.5
E35K	4	1.0 ± 0.2	1 ± 1	+0.5 ± 0.1
E98K	3	0.9 ± 0.1	1.08 ± 0.02	−1.9 ± 0.9

[a]Formation of yeast iso-1 ferricytochrome c(C102T)/rCcP complex in 0.100 M ionic strength DMG buffer, pH 6.0, 20 °C. The reported uncertainties in n, K_{A1}, and $\Delta H^{0\prime}$ are standard deviations of the mean from multiple determinations. [b]n set equal to 1 during fitting to the single-binding-site equation. [c]No detectable interaction under the experimental conditions, see text for details.

Binding of Yeast Iso-1 Ferricytochrome c(C102T) to CcP Charge-Reversal Mutants. Between 2 and 6 ITC titrations were performed for each of the 44 charge-reversal mutations of rCcP included in this study. Representative titrations for all of the mutants are shown in the Supporting Information, Figures S1−S88. Average values for n, K_{A1}, and $\Delta H^{0\prime}$ for each mutant, as well as that of rCcP, are collected in Table S1 of the Supporting Information. Figure 3A,B shows the average values of $\Delta H^{0\prime}$ and $K_{D1} = 1/K_{A1}$ as a function of residue number.

The charge-reversal mutants are arranged into two groups based upon their affinity for yCc. Group 1 includes those mutants that have K_{A1} values that are within a factor of 2 of the value for rCcP. Since factors in the data analysis such as baseline corrections and deviations of the value of n from unity can alter the value of K_{A1} by up to a factor of 2, we use a factor of 2 or more to define a significant change. Thirty-one of the 44 mutants are included in Group 1 including the two positive-to-negative charge-reversal mutants, R31E and K149D. The remaining 13 mutants, those having K_{A1} values more than a factor of 2 smaller than that of rCcP, are included in Group 2 and listed in Table 1.

Group 1 Mutants. The Group 1 mutants have an average value of K_{A1} equal to $(2.8 \pm 0.7) \times 10^5$ M^{-1}, ranging between 1.7×10^5 M^{-1} for D140K and 4.7×10^5 M^{-1} for E214K. The

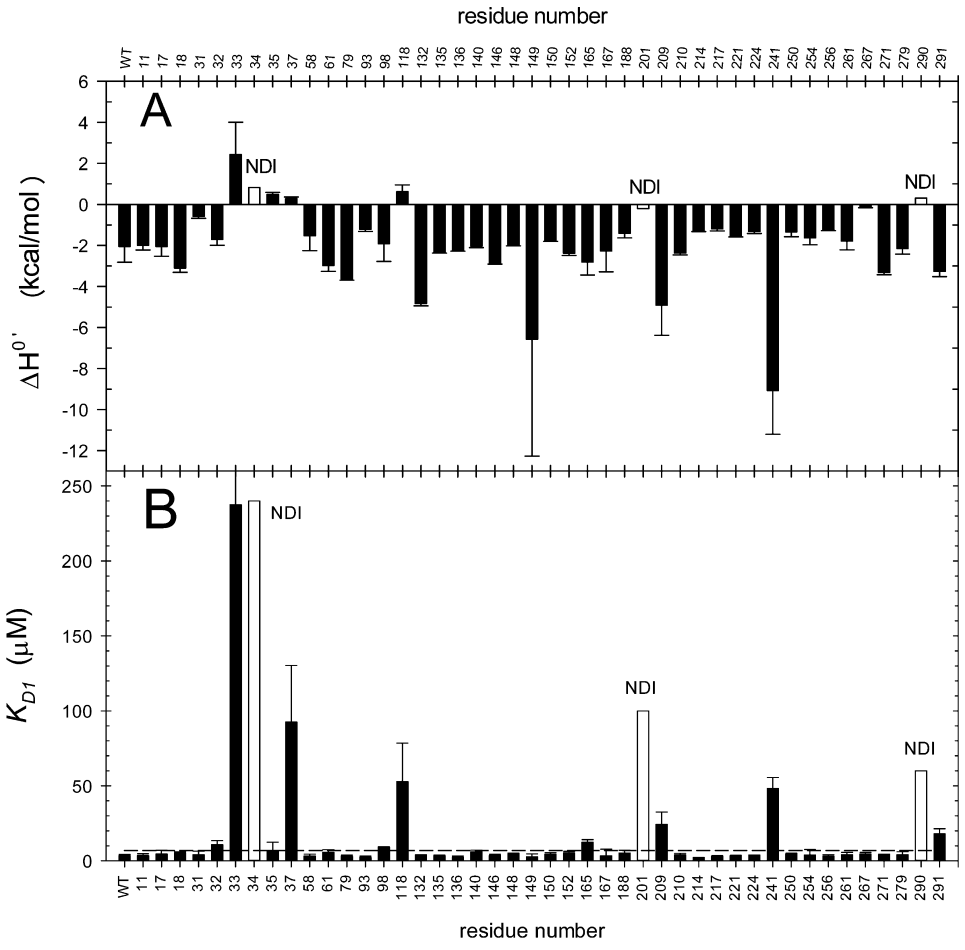

Figure 3. Bar graph showing the average values of $\Delta H^{0\prime}$ (A) and $K_{D1} = 1/K_{A1}$ for the yCc/CcP mutant complexes (B) for wild-type CcP (wt) and each of the 44 charge-reversal mutants used in this study. No detectable interaction was observed for D34K, E201K, and E290K and the estimated values for $\Delta H^{0\prime}$ and K_{D1} for these mutants are shown by open bars (see text for further explanation). The dashed line in panel B represents two-times the value of K_{D1} for the yCc/rCcP complex.

DOI: 10.1021/acs.biochem.5b00686
Biochemistry 2015, 54, 4845−4854

average value of $\Delta H^{0\prime}$ for these mutants is -2 ± 1 kcal/mol, ranging between -7 ± 6 kcal/mol for K149D to -0.12 ± 0.04 kcal/mol for E267K.

Several of the mutants within Group 1 have atypical behavior. E167K has limited solubility in 0.100 M ionic strength buffers. Six titrations were carried out in two different buffer systems, 0.100 M ionic strength DMG buffer and 0.100 M ionic strength potassium phosphate buffer, both at pH 6.0. Saturated solutions of E167K, after dialysis at 4 °C, were 13.6 μM and 18.1 μM in the DMG and potassium phosphate buffers, respectively. Because of the low solubility and associated small thermal peaks, Figure S51, the value of n was fixed at unity for the analysis. The best-fit values for K_{A1} and $\Delta H^{0\prime}$ for the E167K mutant were within experimental error of those for rCcP, Table S1.

In fitting the titration data, the value of n had to be fixed at unity only for E167K within the Group 1 mutants. The average value of n for the other 30 mutants in Group 1 is 1.0 ± 0.2, ranging from 0.47 ± 0.03 for D132K to 1.34 ± 0.08 for R31E. The deviation of n from unity for D132K is the largest observed among the Group 1 mutants and was used to evaluate the effect of n on the values for K_{A1} and $\Delta H^{0\prime}$. Allowing n to vary during the fitting procedure gives average values for n, K_{A1}, and $\Delta H^{0\prime}$ of 0.47 ± 0.03, $(2.7 \pm 0.3) \times 10^5$ M^{-1}, and -4.8 ± 0.1 kcal/mol, respectively, for D132 K. Fixing the value of n at unity and refitting the two D132K titrations gives average values for K_{A1} and $\Delta H^{0\prime}$ of $(1.3 \pm 0.9) \times 10^5$ M^{-1} and -3.1 ± 0.2 kcal/mol, respectively. K_{A1} decreases by 52% and the magnitude of ΔH decreases by 35% as n varies from 0.47 to 1.0.

Because of the similarity of the K_{A1} values for the 31 mutants in Group 1 with that of rCcP, we conclude that the 31 surface sites represented by these mutants do not make significant contributions, within the accuracy of our experiments, to the electrostatic interaction between rCcP and yCc in formation of the 1:1 complex at 0.100 M ionic strength.

Group 2 Mutants. The 13 mutants included in Table 1 decrease the binding affinity for yCc by at least a factor of 2 and are listed in order of increasing affinity for yCc. The Group 2 mutants can be visually broken down into two subgroups, Figure 3B. The first three mutants listed in Table 1, D34K, E201K, and E290K, show no detectable interaction with yCc under the experimental conditions of the ITC experiments. Estimated values (see below) of $K_{D1} = 1/K_{A1}$ and $\Delta H^{0\prime}$ are represented by the open bars in Figure 3. The remaining 10 mutants listed in Table 1 have K_{A1} values that vary from about 73 times smaller than K_{A1} for rCcP, D33K, to about 3 times smaller, E98K. We discuss each of these two subgroups below.

Mutants with No Detectable Interaction with yCc. It is important to emphasize that the reason D34K, E201K, and E290K show no detectable interaction with yCc under the conditions of the ITC experiments is due to weak binding with substantially decreased values of K_{A1} and not due to a vanishingly small value of $\Delta H^{0\prime}$. There is ample evidence in the literature that D34N and E390N, two charge-neutralization mutants, decrease both yCc and hCc binding by factors of 4 or greater,[26−28] and charge-reversal mutations at these sites should decrease the affinity to an even larger extent. At lower ionic strengths, we observe yCc binding to D34K but with a significantly lower affinity than rCcP (see below). All three mutants react rapidly with H_2O_2 with rates similar to that of rCcP, but all three have significantly lowered catalytic activity,[18] strongly suggesting that the reduced activity is due to an altered interaction with yCc. Estimates of the upper-limits for K_{A1} for D34K, E201K, and E290K are made below.

There is no apparent interaction between D34K and yCc during the ITC titration experiments as illustrated in Figures 4

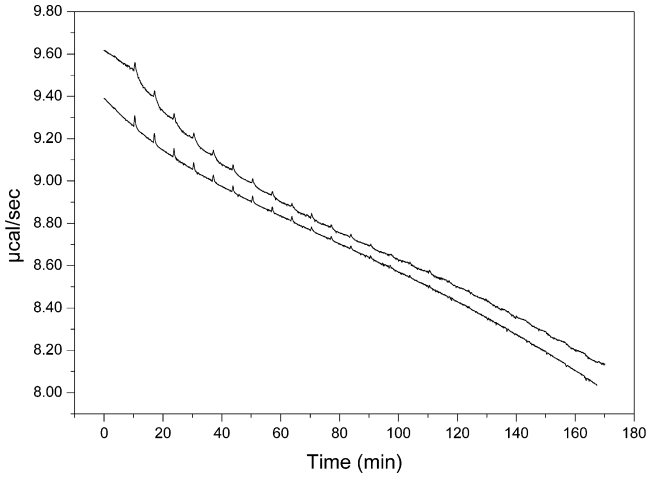

Figure 4. ITC titration of D34K (69.7 μM) with yCc (1.065 mM) (lower trace) and yCc dilution (upper trace). Experimental conditions: 56 mM DMG buffer, pH 6.0, 0.100 M ionic strength, 20 °C.

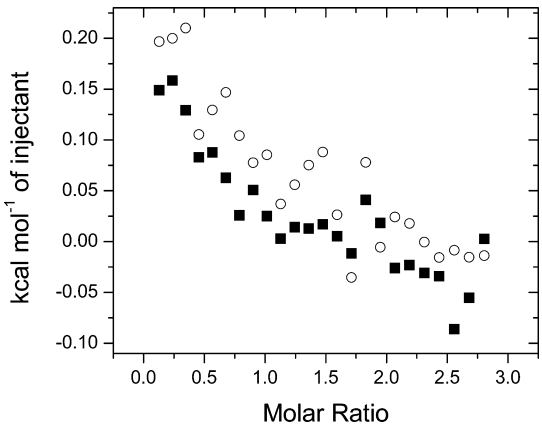

Figure 5. Integrated peak areas for the ITC titration (solid squares) and yCc dilution (open circles) shown in Figure 4. The titration and the dilution peak areas are essentially the same such that no detectable interaction is observed by ITC under the conditions of this experiment. Five additional titrations, using two different isolates of D34K, gave the same results.

and 5. Figure 4 shows a titration using 69.7 μM D34K and 1.065 mM yCc and the corresponding yCc dilution. The integrated peak areas for the titration and dilution are almost identical, Figure 5. Six ITC titrations were carried out using two different isolates of D34K with the same results. In order to demonstrate interaction between yCc and D34K, we have carried out preliminary experiments at lower ionic strength and have detected significant binding in 10 mM DMG buffer, pH 6.0 (0.017 M ionic strength). The values for K_{A1} and $\Delta H^{0\prime}$ for yCc binding to D34K in 10 mM DMG buffer are $(3 \pm 2) \times 10^5$ M^{-1} and $+0.8 \pm 0.3$ kcal/mol, respectively. Wang and Pielak[22] report K_{A1} and ΔH values for yCc binding to rCcP of $(1.0 \pm 0.7) \times 10^8$ M^{-1} and -8.6 ± 0.9 kcal/mol, respectively, in 10 mM DMG, pH 6.0 and 25 °C. Comparing our results for D34K

DOI: 10.1021/acs.biochem.5b00686
Biochemistry 2015, 54, 4845−4854

with the results of Wang and Pielak for rCcP indicates that the binding of yCc to D34K is about 330-fold weaker than binding to rCcP at 0.017 M ionic strength. As the ionic strength is increased to 0.100 M, the difference in yCc affinity between D34K and rCcP should decrease. Assuming that the ionic strength dependence of K_{A1} for D34K is the same as for rCcP,[23] K_{A1} for D34K is estimated to be 1.3×10^3 M^{-1} at 0.100 M ionic strength, about 225-fold smaller than for rCcP. Alternatively, we can estimate an upper limit for K_{A1} of 4×10^3 M^{-1} for the D34K by comparison with the K_{A1} for D33K, Table 1, a mutant that has very weak binding and a positive value of ΔH, similar to that of D34K, but one for which we can evaluate the ITC titration in terms of both K_{A1} and ΔH.

In Figure 3A,B, we indicate the uncertainty of $\Delta H^{0\prime}$ and K_{D1} $(1/K_{A1})$ for yCc binding to D34K at 0.10 M ionic strength by using open bars. We plot the $\Delta H^{0\prime}$ value of +0.8 kcal/mol observed in 10 mM DMG buffer for the yCc/D34K interaction. We also use the larger of the two estimates for the maximum value of K_{A1} at 0.100 M ionic strength for the D34K mutant, 4×10^3 M^{-1}.

As with D34K, we detect no apparent interaction between yCc and the E201K mutant at 0.10 M ionic strength, Figures S55 and S56, Supporting Information. The E201K mutation significantly alters the spectroscopic and catalytic properties of the enzyme.[18] The catalytic activity of E201K is very small. In 0.10 M ionic strength potassium phosphate buffer, pH 7.5, the initial velocities for both rCcP and the E210K mutant follow simple Michaelis−Menten kinetics as a function of the yCc concentration. The Michaelis constant, K_M, for rCcP and E201K are 2.1 ± 0.2 and 2.9 ± 0.9 μM, respectively, and the maximum turnover rates, V_{max}/e_0, for rCcP and the E201K mutant are 640 ± 20 and 2.8 ± 0.2 s^{-1}, respectively. While the K_M values are within experimental error of one another, V_{max}/e_0 for E201K is only 0.4% of that of the native enzyme. Two interpretations of the steady-state kinetic data are possible, both of which suggest significant perturbation of the yCc/E201K complex. Since K_M is a good approximation for K_{D1} in the yCc/rCcP system,[23] one interpretation of the steady-state kinetic data is that yCc binds to E201K with a K_{D1} value similar to that of wild-type rCcP, but that the rate of electron transfer between bound yCc and the Trp-191 radical in CcP Compound I is decreased 230-fold. Alternately, one could assume that only a minor form of the E201K mutant is catalytically active (0.4%), binding yCc with near wild-type affinity, and that more than 99% of the mutant is catalytically inactive due to a very weak binding of yCc.

Glu-201 is adjacent to Ala-193 and Ala-194 on the surface of CcP. Ala-193 and Ala-194 make van der Waals contact with yCc in the 1:1 complex and are thought to be part of the electron transfer pathway from the heme in yCc to the Trp-191 radical in CcP Compound I. Converting Glu-201 to a lysine residue could disrupt the interaction between CcP and yCc, slowing both the rate of electron transfer as well as decreasing the binding affinity.

During the ITC titration of E201K by yCc there is a slight bias toward the titration peaks being more exothermic than the yCc dilution peaks. Estimates of the limits for both K_{A1} and $\Delta H^{0\prime}$ can be made in the following manner. The value of n is fixed at unity. If we assume that K_{A1} equals 3.4×10^5 M^{-1}, as suggested by the steady-state kinetics, and allow only $\Delta H^{0\prime}$ to vary during the fitting procedure we obtain, we obtain an average value for $\Delta H^{0\prime}$ of −0.13 ± 0.10 kcal/mol for the three titrations. This gives an estimate for the maximum value of K_{A1} and a minimum absolute value for $\Delta H^{0\prime}$. On the other hand, if we assume that $\Delta H^{0\prime}$ for the E201K is identical to that for rCcP, −2.1 kcal/mol, refitting the data gives an average value for K_{A1} of 3.3×10^2 M^{-1}. This gives as estimate for the minimum values of K_{A1}. The estimates for K_{A1} vary by 3 orders of magnitude. The geometric mean of the two estimates for K_{A1} is about 1.0×10^4 M^{-1} plus or minus 1.5 orders of magnitude. We have included the geometric mean of the K_{A1} estimates in Figure 3A as an open bar. Using the geometric mean for K_{A1} and refitting the titration data gives a value of −0.2 kcal/mol for $\Delta H^{0\prime}$, Figure 3A.

The third mutant showing no interaction with yCc is E290K. Six ITC were carried out using a single isolate of E290K. The E290K concentrations varied between 46.8 and 110 μM, and the yCc concentrations varied between 0.858 and 1.179 mM. Figure S85 shows one of the titrations along with the dilution of yCc under identical conditions. Figure S86 shows plots of the heats for the titration and dilution shown in Figure S85. The peak areas for the E290K titration and yCc dilution are of the same magnitude.

We have previously investigated the catalytic activity of E290K.[18] In 0.10 M ionic strength potassium phosphate buffer, pH 7.5, the initial velocities of the E290K-catalyzed reaction follow simple Michaelis−Menten kinetics as a function of the yCc concentration. The Michaelis constant for E290 K is 60 ± 11 μM, and the maximum turnover rate, V_{max}/e_0, is 140 ± 10. In terms of the maximum turnover rate, E290K retains 22% of the wild-type enzyme activity. We use the value of K_M to estimate K_{A1}[23] and refit the ITC data to estimate $\Delta H^{0\prime}$ for the interaction of E290K and yCc. Fixing the values of n and K_{A1} at 1.0 and 1.67×10^4 M^{-1}, respectively, the six ITC titrations give ΔH values that range from −0.3 to +1.1 kcal/mol and averages +0.3 ± 0.6 kcal/mol. We have included estimates for K_{A1} and $\Delta H^{0\prime}$ of 1.67×10^4 M^{-1} and 0.3 kcal/mol, respectively, as open bars in Figure 3A,B.

Mutants with a Greater than 2-Fold Decrease in yCc Affinity. The last 10 mutants listed in Table 1 have a 2-fold or greater decrease in yCc affinity compared to rCcP. In general the fit to the single-binding-site model is excellent with the average standard deviation in K_{A1} for the 10 mutants equal to 34% of the mean value of K_{A1}. The average standard deviation for $\Delta H^{0\prime}$ is 32% of the mean value of $\Delta H^{0\prime}$. The value of n had to be fixed at unity during the fitting of the data for D33K and D37K due to the very weak binding for these two mutants. For the remaining eight mutants, the average value of n is 0.8, ranging from 0.4 for E32K to 1.0 for E35K. The deviations of n from unity have little effect on the values of K_{A1} and $\Delta H^{0\prime}$. In the case of E32K, allowing n to vary during the analysis leads to the parameters shown in Table 1. If n is fixed at unity for the analysis of the E32K titrations, the average best-fit values for K_{A1} and $\Delta H^{0\prime}$ are $(0.62 \pm 0.08) \times 10^5$ M^{-1}, a decrease of 24% from the Table 1 value, and $\Delta H^{0\prime} = -2 \pm 1$ kcal/mol, a 5% decrease from the Table 1 value.

DISCUSSION

The 13 mutants listed in Table 1 are the mutants of interest. These are the charge-reversal mutations that decrease the binding affinity for yCc in solution. Eight of the mutations (E32K, D33K, D34K, E35K, E118K, E201K, E290K, and E291K) are within, or immediately adjacent to, the crystallographically defined yCc binding site,[12] Site 1, on the surface of CcP, Figure 6. We define the "front-face" of CcP as the CcP surface surrounding Site 1. Three of the mutants listed in Table

DOI: 10.1021/acs.biochem.5b00686
Biochemistry 2015, 54, 4845−4854

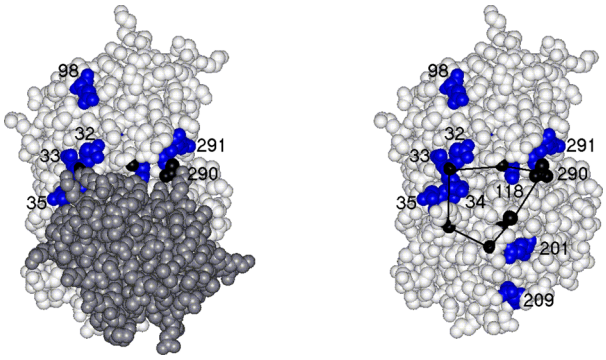

Figure 6. Front-face of CcP in the 1:1 yCc/CcP complex. The data are from the Protein Data Bank entry 2PCC. The left-hand structure shows yCc (gray) bound to the front-face of CcP (white), while the right-hand structure shows CcP in the same orientation with yCc removed. In the right-hand structure, the yCc binding site is identified by the atoms colored in black (unlabeled) and the interconnecting black lines. Only 11 atoms in CcP are within 3.6 Å of bound yCc in the crystal structure and these are located on CcP residues Arg-31, Glu-32, Asn-38, Tyr-39, Ala-193, Ala-194, Val-197, and Glu-290. Table S2 in the Supporting Information lists the specific CcP-yCc interactions. The mutation sites for 10 of the 13 mutants listed in Table 1 are visible in this view. The mutation sites are labeled by their residue number, and the residues are shown in blue. These 10 mutation sites include Glu-32 (the carbonyl oxygen is colored black), Asp-33, Asp-34, Glu-35, Glu-98, Glu-118, Glu-201, Glu-209, Glu-290 (the carboxylate group is colored black), and Glu-291.

1, D37K, E98K, and E209K, are near, but somewhat removed, from Site 1. Although Glu-209 is visible on the front-face of CcP, the lower front surface of CcP falls away from the bound yCc and the carboxylate group of Glu-209 is actually 8.8 Å from the nearest yCc atom when bound at Site 1and 11.0 Å from the nearest yCc charged group, Lys-27. Figures 7 and 8 provide

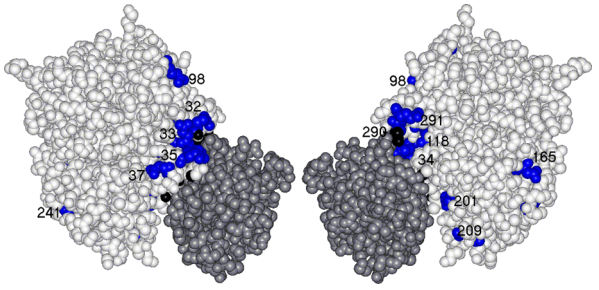

Figure 7. "Left" and "right" faces of CcP. The left-hand structure shows the "left-face" of CcP. The left-hand structure is rotated 90° counterclockwise about a vertical axis relative to the structures shown in Figure 6. The mutation site Asp-37, which is not visible on the front-face of CcP, is seen on the left-face along with a partial view of Asp-241 located on the "back-side" of CcP. The right-hand structure shows the "right-face" of CcP and is rotated 90° clockwise about a vertical axis relative to the structures shown in Figure 6. The mutation sites Glu-201 and Glu-209 are seen relative to bound yCc as well as the mutation site Asp-165, which is toward the back side of CcP.

different perspectives on the location of the E209 K mutation relative to bound yCc. D37K is visible on the "left-face" of CcP, Figure 7. The carboxylate of Asp-37 is 9.4 Å from the nearest atom of yCc bound at Site 1 and 11.5 Å from the nearest charged group, Lys-11. As will be seen later, both Asp-37 and Glu-209 are within the boundary regions of a dynamic encounter complex,[10,24] which is in equilibrium with the

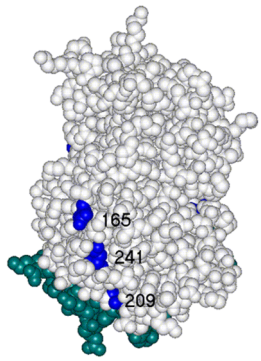

Figure 8. "Back-side" of CcP. This structure is rotated 180° about a vertical axis relative to the structures shown in Figure 6. The mutation sites Asp-165, Asp-241, and a partial view of Asp-209 are shown in this view.

more stable Site 1 complex. The remaining two mutants listed in Table 1, D165K and D241K, are located on the "back-side" of CcP, Figure 8, opposite Site 1.

The results of the current study are consistent with previous site-directed mutagenesis studies that have shown that Asp-33, Asp-34, Asp-37, and Glu-290 influence *Cc* binding, while residues Glu-79, Asp-148, Lys-149, and Asp-217 do not.[17,18,25−31] An important aspect of the current study is that the entire surface of CcP has been investigated, evaluating the influence of each negatively charged site on its interaction with yCc. The current study adds an additional nine carboxylates to the previously identified four that affect *Cc* binding (Glu-32, Glu-35 Glu-98, Glu-118, Asp-165, Glu-201, Glu-209, Asp-241, Glu-291) and, just as important, adds an additional 28 acidic residues to the list of residues that do not affect yCc binding.

The crystallographic structure of the yCc/CcP complex, Figures 6 and 7, gives a static view of the complex. There is ample evidence in the literature that the 1:1 complex is dynamic in nature.[11,13,15,32−34] Recent NMR studies indicate that the 1:1 complex in solution can be described as an equilibrium mixture of a dominant well-defined form, similar to the crystallographic structure and accounting for about 70% of the complex, and a more dynamic encounter complex characterized by the interaction of yCc over an extended region of the CcP surface accounting for the remaining 30% of the 1:1 complex.[15,24,34−36]

Volkov, Ubbink, and colleagues have made resonance assignments for essentially all of the backbone amide groups (^{1}H and ^{15}N) in CcP and cyanoCcP by using isotopically enriched CcP.[36,37] The chemical shifts of the amide resonances are sensitive to the chemical environment, and, upon binding of yCc at high ionic strength, where only 1:1 complex formation is expected, significant changes in the chemical shift positions of a number of the CcP amide groups have been observed.[36−38] The size of the chemical shifts is related to the lifetime of the complex, and the largest chemical shifts indicate that yCc occupies a single orientation within the complex for a significant fraction of the time. The largest shifts occur for residues Ala-193 to Asn-196, consistent with yCc binding to Site 1, with smaller shifts observed for residues significantly away from Site 1, including Leu-182, Glu-209, and Trp-211, indicating an interaction over an extended surface area of CcP.

The encounter complex has been characterized by using paramagnetic relaxation enhancement (PRE) NMR techniques

DOI: 10.1021/acs.biochem.5b00686
Biochemistry 2015, 54, 4845−4854

to map weak interactions between yCc and CcP.[15,24,34−36] In the PRE NMR experiments, paramagnetic spin labels are covalently attached to specific sites on one of the two interacting proteins, and the effect of the spin label on the second protein is investigated. The unpaired electron on the spin label increases the relaxation rate of nearby nuclei due to magnetic dipolar interactions leading to peak broadening in the NMR spectrum. The effect is dependent upon the inverse sixth power of the distance between the unpaired electron and the nucleus. The effect is strong at short distances and can be used to detect weakly populated states near the spin label. In initial experiments, PRE effects on the NMR spectrum of yCc were determined for 10 different spin-labeled CcP molecules.[15,34] When the spin label was located near the crystallographic binding site on CcP (CcP residues 38, 200, and 288), significant yCc PREs were observed, and when the spin labels were located elsewhere on the CcP surface (CcP residues 97, 137, 141, 164, 213, and 263) no PRE effects on yCc were observed. Later studies using spin-labeled yCc to monitor CcP-detected PREs found that the encounter complex extended over five different regions on the CcP surface, residues 30−42, 144−154, 176−231, 252−261, and 287−293 (see Figure 3 of ref 24). The affected regions involve about 33% of the 294 residues in CcP and include a small region on the back-side of CcP, residues 144−154, directly opposite Site 1.

In the following discussion we utilize the latest NMR studies[24] to define five subregions of the encounter complex. Three of the subregions overlap Site 1 and two do not. EC1 is defined as CcP residues 30−42 and overlaps the upper left-hand corner of Site 1, Figure 6. EC2 is defined as residues 176−231, which is a large region toward the bottom of the front and left faces of CcP and has a significant overlap with Site 1, Figures 6 and 7. EC3 is defined as residues 287−293 and overlaps the upper right-hand side of Site 1, Figure 6. EC4 includes residues 252−261, located toward the middle back of the right face of CcP, Figure 7, and does not overlap site 1. EC5 includes CcP residues 144−154 and is located on the backside of CcP, Figure 8, furthest removed from Site 1.

Using a multisite model to characterize yCc binding to CcP, K_{A1} can be expressed as a sum of terms involving binding to Site 1 and the five subregions of the encounter complex, eq 2. K_{Site1} is the equilibrium association constant for binding to Site 1, and K_{ECi}, with indices 1

$$K_{A1} = K_{Site1} + \sum_{i=1}^{5} K_{ECi} \quad (2)$$

through 5, are the equilibrium association constants for the binding of yCc to the five defined subregions of the encounter complex. Under the conditions of the ITC experiments, K_{Site1} = 2.0×10^5 M^{-1} and $\sum_{i=1}^{5} K_{ECi} = 0.9 \times 10^5$ M^{-1}, using the estimate from the PRE NMR experiments that about 70% of the 1:1 complex has yCc bound to Site 1 and 30% bound in the encounter complex. Any mutation that decreases the binding affinity by more than 30% necessarily requires that the mutation affect binding at Site 1. All 13 mutants in Table 1 decrease the binding affinity for yCc by at least 63%, indicating that all influence yCc binding at Site 1.

Mapping the 13 mutants in Table 1 into the five encounter complex subregions shows that five of the mutants map into EC1 (E32K, D33K, D34K, D35K, and D37K), two map into EC2 (E201K, E209K), two map into EC3 (E290K, E291K), and none map into EC4 or EC5. Four of the Table 1 mutants do not map into any of the currently defined subregions of the encounter complex (E98K, E118K, D165K, and D241K).

In light of the PRE NMR studies, which suggest that about 30% of the 1:1 complex is a dynamic encounter complex where yCc binds over an extended region of the surface of CcP, it is interesting to observe that single-site, charge reversal mutations (D34K, E201K, and E290K) can essentially eliminate yCc binding at 0.10 M ionic strength, while two others (D33K and D37K) inhibit yCc binding by more than 96%, Table 1. The simplest interpretation of the data is that less than 4% of yCc binding occurs in regions that are not influenced by the electrostatic potential generated by the residues at positions 33, 34, 37, 201, and 290. The ITC data suggest that the most populated regions of the encounter complex are those that overlap Site 1.

There is a distinctly negative patch on the surface of CcP where five of six residues have carboxylate groups, Glu-32, Asp-33, Asp-34, Glu-35, and Asp-37. The ITC study emphasizes the importance of this region in binding yCc. Charge-reversal mutations at each of the five carboxylates decrease the affinity for yCc, Table 1 and all five residues are within, or near, the crystallographically defined yCc binding site, Figures 6 and 7. They are also all in region EC1 of the encounter complex. The ITC data provide some evidence that binding of yCc at Site 1 in solution may not be identical to binding of yCc to Site 1 in the crystal structure. If we look at the distance between the carboxylate group of each residue with the nearest lysine ε-amino group in yCc bound to Site 1 in the crystal structure, the order of mutants is terms of increasing distance is D34K (3.8 Å to Lys-87), E32K (5.1 Å to Lys-87), E35K (5.2 Å to Lys-5), D33K (7.1 Å to Lys-87), and D37K (11.5 Å to Lys-11). The order of mutants in terms of decreasing yCc affinity (lowest to highest) is D34K, D33K, D37K, D32K, and D35K, Table 1. Both D32K and D35K decrease the yCc binding affinity to a lesser extent than expected based on the relative locations of their carboxylates in the crystal structure of the yCc-CcP complex compared to D34K, D33K, and D37K. One interpretation, based on the PRE NMR experiments, is that in solution yCc bound to CcP is relatively mobile and that the time-averaged interaction of yCc with Asp-32 and Asp-35 is less than with the other three carboxylates in this cluster, suggesting a slightly different orientation between crystal and solution.

Perhaps the most intriguing aspect of the current study is that D165K and D241K decrease yCc binding by 72% and 93%, respectively, Table 1, indicating that both decrease yCc binding at Site 1. Asp-165 and Asp-241 are located on the back side of CcP, Figure 8, and the carboxylate groups of both are about 30 Å from the nearest charged-residue in yCc (Lys-72) when yCc is bound to Site 1. Why D165K and D241K decrease yCc binding to a greater extent than E32K, E35K, and E98K is unclear since the charge-reversal sites in the latter mutants are much closer to Site 1-bound yCc than the charge-reversal sites in D165K and D241K. D241K even decreases yCc binding more than E209K and E291K.

In the case of D241K, there may be other reasons besides electrostatic repulsion for the decreased yCc binding affinity. In addition to having an almost 14-fold decrease in yCc binding affinity, the observed heat of interaction for formation of the yCc/D241K complex is −9 kcal/mol, the most exothermic heat of interaction observed for the 44 mutants, and more than 4 times larger than that of rCcP. Previously we have found that D241K has a UV−vis spectrum characteristic of a predominantly six-coordinate heme at pH 6, it has less than 5% of wild-

DOI: 10.1021/acs.biochem.5b00686
Biochemistry 2015, 54, 4845−4854

type catalytic activity for oxidation of yCc^{2+}, and CcP Compound I formation is not detected when the mutant reacts with hydrogen peroxide.[18] Further characterization of the D241K mutant shows that its room temperature CD spectrum is similar to that of rCcP, Figure S89, but that its thermal denaturation isotherm is distinctly different, Figure S90. At pH 6.0, in 0.100 M ionic strength potassium phosphate buffer, rCcP denatures in a single, cooperative transition with a midpoint temperature, T_m, of 59 ± 1 °C and a breadth of 5.6 °C (10% to 90% denaturation). Under the same conditions, T_m for D241K is 53.0 ± 0.6 °C, and the breadth of the transition is 14 °C. The D241K mutation decreases the thermal stability of the protein significantly. The breadth of the D241K transition indicates that the thermal denaturation is less cooperative than that of rCcP and suggests that the mutant could exist in a number of rapidly interconverting protein conformers, each with different thermal stability. If different D241K conformers exist at 20 °C, some may have reduced affinity for yCc providing another mechanism for decreasing the overall yCc affinity in this mutant. There is evidence that different protein conformers can influence yCc binding. Sterckx and Volkov[39] have shown that apoCcP has very similar structural and hydrodynamic properties as those of holoCcP yet apoCcP does not bind Cc. ApoCcP is slightly more expanded than holoCcP in solution, exhibiting some of the characteristics of a molten globule state, and apparently the expanded or dynamic nature of apoCcP disrupts Cc binding.

A mechanism to explain the reduced affinity of the D241K mutant for yCc is shown in eq 3, where P_i and P represent inactive and native-like conformations, respectively, of D241K.

$$P_i + yCc \underset{K_c}{\overset{\Delta H_c^{0'}}{\rightleftharpoons}} P + yCc \underset{K_{A1}}{\overset{\Delta H_b^{0'}}{\rightleftharpoons}} yCc\text{-}P \quad (3)$$

Under the assumption that yCc only binds to the native-like conformation of D241K, the apparent association constant is given by $K_{A1}^{app} = K_c K_{A1}$ and the enthalpy of the reaction is given by $\Delta H^{0'} = \Delta H_c^{0'} + \Delta H_b^{0'}$. If the conformational equilibrium has a K_c value of 0.072 and a $\Delta H_c^{0'}$ value of −6.9 kcal/mol, binding of yCc to the native-like conformation of D241K would be identical to that of rCcP.

Although a mechanism such as that shown in eq 3 could be applied to all of the mutants, the simplest interpretation of the data is to assume that the charge-reversal mutations only alter the electrostatic field of CcP and not the conformation of the enzyme. This is based on the observation that 31 of the 44 mutants included in this study have no significant effect on yCc binding, most of the mutants have UV−vis spectra similar to that of rCcP at pH 6,[18] and most retain significant catalytic activity.[18] Only in the event that there is some evidence that a mutant may exist in alternate conformational states, such as the altered heme-ligation and thermal denaturation shown by D241K, would a mechanism like that shown in eq 3 need to be considered.

In conclusion, neither of the extreme models for the binding of Cc to CcP presented in the introduction is entirely correct,[5,13−15] but elements of both contribute to our current understanding of the binding of Cc to CcP. The 1:1 complex is formed by electrostatic attraction between the two proteins to produce a very dynamic encounter complex that samples a relatively large area on the surface of CcP.[15,24,34−36] The encounter complex facilitates the rapid formation and dissociation of a more stable electron-transfer active complex, with yCc bound at or near Site 1.[12] The current study is consistent with this model and provides some constraints on the populations of the various subregions of the encounter complex. The charge-reversal mutations suggest that those regions of the encounter complex that overlap Site 1 (EC1, EC2, and EC3) are the most populated, and relatively little yCc is bound in regions EC4 and EC5 of the encounter complex.

■ ASSOCIATED CONTENT

Supporting Information

The Supporting Information is available free of charge on the ACS Publications website at DOI: 10.1021/acs.biochem.5b00686.

Representative traces of the unprocessed isothermal calorimetric titrations for all 44 charge-reversal mutants as well as the fitting of the corrected data to the one-binding-site model are shown in Figures S1−S88. The best-fit values for n, K_{A1}, and $\Delta H^{0'}$ obtained from the titrations of rCcP and the 44 CcP charge-reversal mutants are collected in Table S1. Figures S89 and S90 show the CD spectra and the thermal denaturation isotherms for rCcP and D241K (PDF)

■ AUTHOR INFORMATION

Corresponding Author

*Phone: (815) 753-6867; fax: (815) 753-4802; e-mail: jerman@niu.edu.

Funding

This work was supported by National Institutes of Health Grant R15-GM59740 to J.E.E.

Notes

The authors declare no competing financial interest.

■ ACKNOWLEDGMENTS

We thank Professor James Satterlee (deceased), Washington State University, for providing the plasmid containing the gene for rCcP and Professor Gary Pielak, University of North Carolina, for providing the plasmid containing the yeast iso-1 cytochrome *c*(C102T) and heme lyase genes.

■ ABBREVIATIONS

CcP, cytochrome *c* peroxidase from any source; yCcP, CcP isolated from Baker's yeast; rCcP, recombinant CcP expressed in *Escherichia coli* with exact sequence as yCcP; *Cc*, cytochrome *c*; Cc^{2+}, ferrocytochrome *c*; Cc^{3+}, ferricytochrome *c*; yCc, recombinant yeast iso-1 cytochrome *c*(C102T); hCc, horse heart cytochrome *c*; ITC, isothermal titration calorimetry; DMG, dimethylglutaric acid; EC1 to EC5, encounter complex subregions 1 to 5

■ REFERENCES

(1) Yonetani, T. (1965) Cytochrome c peroxidase. II. Stoichiometry between enzyme, H_2O_2, and ferrocytochrome *c*, and enzymatic determination of extinction coefficient of cytochrome *c*. *J. Biol. Chem. 240*, 4509−4514.

(2) Coulson, A. F. W., Erman, J. E., and Yonetani, T. (1971) Studies on cytochrome *c* peroxidase: XVII. Stoichiometry and mechanism of the reaction of compound ES with donors. *J. Biol. Chem. 246*, 917−924.

(3) Kang, C. H., Ferguson-Miller, S., and Margoliash, E. (1977) Steady state kinetics and binding of eukaryotic cytochromes *c* with yeast cytochrome *c* peroxidase. *J. Biol. Chem. 252*, 919−926.

DOI: 10.1021/acs.biochem.5b00686
Biochemistry 2015, 54, 4845−4854

(4) Mauk, M. R., Ferrer, J. C., and Mauk, A. G. (1994) Proton linkage in formation of the cytochrome *c*-cytochrome *c* peroxidase complex: electrostatic properties of the high- and low-affinity cytochrome binding sites of the peroxidase. *Biochemistry 33*, 12609−12614.
(5) Erman, J. E., and Vitello, L. B. (2002) Yeast cytochrome *c* peroxidase: mechanistic studies via protein engineering. *Biochim. Biophys. Acta, Protein Struct. Mol. Enzymol. 1597*, 193−220.
(6) Poulos, T. L., Freer, S. T., Alden, R. A., Edwards, S. L., Skoglund, U., Takio, K., Eriksson, B., Xuong, N.-h., Yonetani, T., and Kraut, J. (1980) The crystal structure of cytochrome *c* peroxidase. *J. Biol. Chem. 255*, 575−580.
(7) Finzel, B. C., Poulos, T. L., and Kraut, J. (1984) Crystal structure of yeast cytochrome *c* peroxidase refined at 1.7 Å resolution. *J. Biol. Chem. 259*, 13027−13036.
(8) Poulos, T., and Kraut, J. (1980) A hypothetical model of the cytochrome *c* peroxidase-cytochrome *c* electron transfer complex. *J. Biol. Chem. 255*, 10322−10330.
(9) Kraut, J. (1981) Molecular geometry of cytochrome *c* and its peroxidase: a model for biological electron transfer. *Biochem. Soc. Trans. 9*, 197−204.
(10) Poulos, T. L., and Finzel, B. C. (1984) Heme enzyme structure and function. *Peptide Protein Rev. 4*, 115−171.
(11) Northrup, S. H., Boles, J. O., and Reynolds, J. C. L. (1988) Brownian dynamics of cytochrome *c* and cytochrome *c* peroxidase association. *Science 241*, 67−70.
(12) Pelletier, H., and Kraut, J. (1992) Crystal structure of a complex between electron transfer partners, cytochrome *c* peroxidase and cytochrome *c*. *Science 258*, 1748−1755.
(13) Nocek, J. M., Zhou, J. S., De Forest, S., Priyadarshy, S., Beratan, D. N., Onuchic, J. N., and Hoffman, B. M. (1996) Theory and practice of electron transfer within protein-protein complexes: Application to the multidomain binding of cytochrome *c* by cytochrome *c* peroxidase. *Chem. Rev. 96*, 2459−2489.
(14) Kang, A., Marjavaara, P. J., and Crane, B. R. (2004) Electron transfer between cytochrome *c* and cytochrome *c* peroxidase in single crystals. *J. Am. Chem. Soc. 126*, 10836−10837.
(15) Volkov, A. N., Worrall, J. A. R., Holtzmann, E., and Ubbink, M. (2006) Solution structure and dynamics of the complex between cytochrome *c* and cytochrome *c* peroxidase determined by paramagnetic NMR. *Proc. Natl. Acad. Sci. U. S. A. 103*, 18945−18950.
(16) Takio, K., Titani, K., Ericsson, L. H., and Yonetani, T. (1982) The primary structure of yeast cytochrome c peroxidase, in *Peroxidases Related Redox Systems, Proceedings of the 3rd International Symposium* (King, T. E., Mason, H. S., and Morison, M., Eds.) pp 625−638.
(17) Pearl, N. M., Jacobson, T., Arisa, M., Vitello, L. B., and Erman, J. E. (2007) Effect of single-site charge-reversal mutations on the catalytic properties of yeast cytochrome *c* peroxidase: Mutations near the high-affinity cytochrome c binding site. *Biochemistry 46*, 8263−8272.
(18) Pearl, N. M., Jacobson, T., Meyen, C., Clementz, A. G., Ok, E. Y., Choi, E., Wilson, K., Vitello, L. B., and Erman, J. E. (2008) Effect of single-site charge-reversal mutations on the catalytic properties of yeast cytochrome *c* peroxidase: Evidence for a single, catalytically active, cytochrome c binding domain. *Biochemistry 47*, 2766−2775.
(19) Goldberg, R. N., Kishore, N., and Lennen, R. M. (2002) Thermodynamic quantities for the ionization reactions of buffers. *J. Phys. Chem. Ref. Data 31*, 231−370.
(20) Wiseman, T., Williston, S., Brandts, J. F., and Lin, L. N. (1989) Rapid measurement of binding constants and heats of binding using a new titration calorimeter. *Anal. Biochem. 179*, 131−137.
(21) Bevington, P. R. (1969) *Data Reduction and Error Analysis in the Physical Sciences*; McGraw-Hill, New York, NY.
(22) Wang, X., and Pielak, G. J. (1999) Equilibrium thermodynamics of a physiologically-relevant heme-protein complex. *Biochemistry 38*, 16876−16881.
(23) Nakani, S., Vitello, L. B., and Erman, J. E. (2006) Characterization of four covalently-linked yeast cytochrome *c*/cytochrome *c* peroxidase complexes: Evidence for electrostatic interaction between bound cytochrome *c* molecules. *Biochemistry 45*, 14371−14378.
(24) Van de Water, K., van Nuland, N. A. J., and Volkov, A. N. (2014) Transient protein encounter characterized by paramagnetic NMR. *Chem. Sci. 5*, 4227−4236.
(25) Corin, A. F., McLendon, G., Zhang, Q., Hake, R. A., Falvo, J., Lu, K. S., Ciccarelli, R., and Holzschu, D. (1991) Effects of surface amino acid replacement in cytochrome *c* peroxidase on complex formation with cytochrome *c*. *Biochemistry 30*, 11585−11595.
(26) Liu, R. Q., Hahm, S., Miller, M., Durham, B., and Millett, F. M. (1995) Photooxidation of Trp-191 in cytochrome *c* peroxidase by ruthenium-cytochrome *c* derivatives. *Biochemistry 34*, 973−983.
(27) Miller, M. A. (1996) A complete mechanism for steady-state oxidation of yeast cytochrome *c* by cytochrome *c* peroxidase. *Biochemistry 35*, 15791−15799.
(28) Erman, J. E., Kresheck, G. C., Vitello, L. B., and Miller, M. A. (1997) Cytochrome *c*/cytochrome *c* peroxidase complex: Effect of binding-site mutations on the thermodynamics of complex formation. *Biochemistry 36*, 4054−4060.
(29) Zhou, J. S., Tran, S. T., McLendon, G., and Hoffman, B. M. (1997) Photoinduced electron transfer between cytochrome *c* peroxidase(D37K) and Zn-substituted cytochrome *c*: Probing the two-domain binding and reactivity of the peroxidase. *J. Am. Chem. Soc. 119*, 269−277.
(30) Leesch, V. W., Bujons, J., Mauk, A. G., and Hoffman, B. M. (2000) Cytochrome *c* peroxidase - cytochrome *c* complex: Locating the second binding domain on cytochrome *c* peroxidase with site-directed mutagenesis. *Biochemistry 39*, 10132−10139.
(31) Pielak, G. J., and Wang, X. (2001) Interactions between yeast iso-1-cytochrome *c* and its peroxidase. *Biochemistry 40*, 422−428.
(32) Poulos, T. L., Sheriff, S., and Howard, A. J. (1987) Cocrystals of yeast cytochrome *c* peroxidase and horse heart cytochrome *c*. *J. Biol. Chem. 262*, 13881−13884.
(33) Gabdoulline, R. R., and Wade, R. C. (2001) Protein-protein association: Investigation of factors influencing association rates by Brownian dynamics simulations. *J. Mol. Biol. 306*, 1139−1155.
(34) Bashir, Q., Volkov, A. N., Ullmann, G. M., and Ubbink, M. (2010) Visualization of the encounter ensemble of the transient electron transfer complex of cytochrome *c* and cytochrome *c* peroxidase. *J. Am. Chem. Soc. 132*, 241−247.
(35) Volkov, A. N., Ubbink, M., and van Nuland, N. A. J. (2010) Mapping the encounter state of a transient protein complex by PRE NMR spectroscopy. *J. Biomol. NMR 48*, 225−236.
(36) Schilder, J., Löhr, F., Schwalbe, H., and Ubbink, M. (2014) The cytochrome *c* peroxidase and cytochrome *c* encounter complex: The other side of the story. *FEBS Lett. 588*, 1873−1878.
(37) Volkov, A. N., Wohlkonig, A., Soror, S. H., and van Nuland, N. A. J. (2013) Expression, purification, characterization, and solution NMR study of highly deuterated yeast cytochrome *c* peroxidase with enhanced solubility. *Biochemistry 52*, 2165−2175.
(38) Volkov, A. N., and van Nuland, N. A. J. (2013) Solution NMR study of the yeast cytochrome *c* peroxidase: cytochrome *c* interaction. *J. Biomol. NMR 56*, 255−263.
(39) Sterckx, Y. G. J., and Volkov, A. N. (2014) Cofactor-dependent structural and binding properties of yeast cytochrome *c* peroxidase. *Biochemistry 53*, 4526−4536.

DOI: 10.1021/acs.biochem.5b00686
Biochemistry 2015, 54, 4845−4854